Urban DEM Generation from Raw Lidar Data: A Labeling Algorithm and its Performance

Jie Shan and Aparajithan Sampath

Abstract

This paper addresses the separation of ground points from raw lidar data for bald ground digital elevation model (DEM) generation in urban areas. This task is considered to be a labeling process through which a lidar point is labeled as either a ground point or a non-ground point. Mathematical formulation is presented to define the ground. A new approach is proposed that conducts one-dimensional labeling in two opposite directions followed by a linear regression, both along the lidar scan line profile. The study shows that the one-dimensional characteristic makes the calculation efficient, and the reliability is assured by the bidirectional labeling process. Lidar data over suburban and downtown Baltimore (Maryland), Osaka (Japan), and Toronto (Canada) are used for the study. Quality assessment is designed and conducted to investigate the performance of the labeling approach by using manually-selected ground truth. It is shown that 2.7 percent ground points are wrongly labeled as building points, and 2.6 percent building points are mistakenly labeled as ground points over the four study areas. Detailed graphic and numerical results are provided to illustrate the proposed labeling approach and its performance for complex urban areas.

Introduction

Lidar (LIght Detection And Ranging) is a remote sensing technique based on laser technology. It measures the two-way travel time of the emitted laser pulses to determine the distance between the sensor and the ground (Wehr and Lohr, 1999). Combined with a Global Positioning System (GPS) and an Inertial Measurement Unit (IMU), lidar can generate a three-dimensional (3D) dense, geo-referenced point clouds for the reflective terrain surface. Compared to the traditional photogrammetric approach, lidar is less dependent on the weather, season, and time of the day in data collection, and can generate 3D topographic surface information more rapidly (Ackermann, 1999; Balsavias, 1999). Despite this advantage, however, lidar measurements are not selective. The original lidar data consist of tremendous points returned from all possible reflective terrain objects, including (bald) ground, buildings, bridges, vehicles, trees, and other non-ground features. For many topographic, hydrographic, agricultural, and construction applications, the non-ground returns must be detected, separated, and removed in order to generate the (bald) digital elevation model (DEM) (Fowler, 2001, pp. 208–236).

This paper will focus on the DEM generation over urban areas from raw lidar point data. In the following section, a literature review on different methodologies developed in recent years is presented based on their assumptions about the ground. The Test Data section describes the four test data sets used in this study. In the Labeling section, the labeling approach is introduced and graphically illustrated. It labels each lidar point (return) as either ground or non-ground point based on the computation result along the one-dimensional (1D) lidar profile. Characteristics of this 1D profile-based labeling approach are discussed. Results of four urban areas (suburban and downtown Baltimore, Osaka, and Toronto) with dense and complex buildings and other urban features are presented in the Results and Assessment section to demonstrate the properties and performance of the proposed labeling approach. Also presented in this section is a comprehensive quantitative evaluation on the performance of the algorithm based on manually selected ground truth in the four data sets. A summary of the paper is presented in the final section as concluding remarks.

What is the Ground?—A Literature Review

The process of eliminating non-ground points from the entire lidar data to obtain ground points is often referred as *filtering* (Vosselman, 2000). Although a variety of different methods have been proposed for this task, all of them essentially need to answer, either explicitly or implicitly, a fundamental question: *what is the ground?* For the convenience of reviewing and comparison, this paper groups the filtering techniques into two general categories, labeling approach and adjustment approach. The following presents a brief review on these approaches in terms of the way they address this fundamental question.

A labeling approach detects the ground points using certain operators. An operator distinguishes ground points from non-ground points based on the output of its calculation. Different labeling approaches have been proposed and implemented. As one of the early efforts, Lindenberger (1993) introduces mathematical morphologic operators for this task. In this approach, an opening operator with horizontal structure element is first used to detect possible ground points. Points within a certain vertical distance to the estimated local average elevation are defined as ground points. An auto-regression process is then followed to refine the initial results obtained from the morphologic operation. Noticing this algorithm is vulnerable to the size of the structure element, Kilian, *et al.* (1996) uses a series of morphologic operators with different sizes to find out the ground. To consider the local relief, Vosselman (2000) proposes a slope-based filter which is shown to be closely related to the erosion operator in mathematic morphology. In this approach, the ground is essentially defined as points that are within a given slope range. Training may be needed to determine the parameters when implementing this filtering process (Vosselman, 2000). In addition to

Geomatics Engineering, School of Civil Engineering, Purdue University, 550 Stadium Mall Drive, West Lafayette, IN 47907-2051 (jshan@ecn.purdue.edu).

Photogrammetric Engineering & Remote Sensing
Vol. 71, No. 02, February 2005, pp. 217–226.

0099-1112/05/7102–0217/$3.00/0

these morphology-based or –related operators, terrain slope (Axelsson, 1999; Sithole, 2001; Yoon and Shan, 2001) and local elevation difference (Wang, *et al.*, 2001) are also used as criteria for DEM generation. Haugerud and Harding (2001) uses a de-spike algorithm to remove forest coverage in lidar data. Based on the assumption that smoothness is a property of the ground surface, the algorithm searches for aberration points where strong local curvature occurs and then removes these points. Similar work is reported by (Raber, *et al.*, 2002) that uses an adaptive point removal process to extract accurate DEM under vegetation coverage.

Ground points can also be identified through an adjustment process. A mathematical function, usually selected as a two-dimensional (2D) polynomial surface, can be used to approximate the ground. In this approach, ground is essentially represented as a continuous or at least a piecewise continuous surface. Points within a certain vertical distance above the surface are treated as ground points. Least squares adjustment is used to detect the non-ground points as if they were blunders by reducing their weights in each iteration calculation. Typical methods of this kind are proposed by (Kraus and Pfeifer, 1998, 2001; Schickler and Thorpe, 2001) based on classical surface modeling and recently by (Elmqvist, 2002) based on active shape modeling.

Most of the above approaches limit their processing within a 2D neighborhood of a lidar point or a subset of the lidar points. Finding and storing such neighborhood proximity requires a significantly large amount of computation and memory because of the large volume of lidar data and their irregular sampling pattern. To facilitate the computation a Triangulated Irregular Network (TIN) is used by (Axelsson, 2000; Haugerud and Harding, 2001; Vosselman, 2000; Vosselman and Mass, 2001) to determine the filter proximity and consider the discontinuity in the terrain surface.

Despite the above reviewed studies and the fact that DEM products can be prepared from many lidar service providers, difficulties still remain in this task. The DEM generation from lidar data is not yet mature (Vosselman and Maas, 2001). Interactive evaluation and manual editing is still a necessary and inevitable step for DEM generation in practice (Petzold, *et al.*, 1999; Knabenschuh and Petzold, 1999). To obtain reliable and accurate DEM products for different complexity of topography is still one primary topic in academia and industry as reflected in recent publications (Crombaghs, *et al.*, 2002; Fowler, 2001; Masaharu and Ohtsubo, 2002; Sithole, 2002). Further efforts are needed to handle complex urban areas. Efficient algorithms are also needed to relieve the need on 2D proximity neighborhood in the calculation. Moreover, we still need a comprehensive understanding on the performance of the filtering process and the quality of the resultant DEM, which have been rarely studied until recently (Crombaghs, *et al.*, 2002; Huising and Gomes Pereira, 1998; Sithole, 2002). Our study is motivated by the above observations and will address most of the issues.

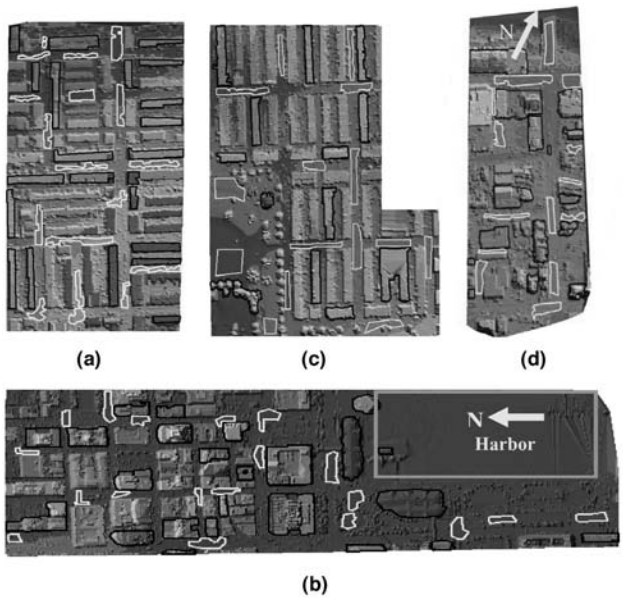

Figure 1. Lidar surface elevation maps and selected ground truth for assessment: (a) Suburban Baltimore, (b) Downtown Baltimore, (c) Osaka, and (d) Toronto. Dark polygons: buildings; light polygons: ground. The figures are not to exact scale.

Test Data

Four airborne lidar data sets are used in this study, and their coded elevation maps are shown in Figure 1. The first two data sets were collected by EarthData Technologies and cover suburban and downtown Baltimore, Maryland, respectively. Suburban Baltimore (Figure 1a) mostly has trees, vehicles, and long buildings with flat roofs. Downtown Baltimore (Figure 1b) is covered densely by tall buildings with complex roofs. Its non-ground features include bridges, vehicles, and trees. Besides, this data set has a harbor where only ships and decks in the water returned lidar signals. The third and fourth data sets are respectively for Osaka, Japan and Toronto, Canada, provided by Optec, Inc. The Osaka data set (Figure 1c) consists of trees, and mostly long and flat buildings. The Toronto data (Figure 1d) are full of tall and complex buildings and other typical urban features.

Table 1 summarizes the properties of the four data sets; the total number of lidar points used in our study is listed, and these points are a portion of the entire data sets. The dimensions of the study area is given by the number of points across track (scanning direction) and along track (flight direction).

TABLE 1. PROPERTIES OF THE TEST LIDAR DATA SETS

Site Name	Baltimore Suburb	Baltimore Downtown	Osaka	Toronto
Total points #	30,000	50,000	50,000	50,000
Dimension (across * along track, in square meters)	~548 * 312	~1,216 * 405 (minus 101,660 water)	~500 * 400 (minus 32,958 no data area)	~167 * 420
Percentile ground slope (5%, 50%, 95% in deg.)	0.2; 2.7; 18.7	0.2; 1.6; 15.8	0; 1.6; 10.7	0; 2.7; 44.3
Ground spacing (across/along track, in meters.)	2.3/4.5	2.5/4.0	1.6/1.7	1.0/1.5
Point density (points/ 10 square meters)	1.8	1.3	3.0	7.2
Labeled ground points #	13,802	25,089	26,416	25,821

It is noted that the Baltimore downtown and Osaka data sets contain a no-data or no-return region as shown in Figure 1b and 1c, respectively. To characterize the topographic relief of the study areas, we list the 5, 50 (median) and 95 percentiles of the ground slope in the study sites. It is shown that Toronto area has very complex topography with a ground slope range of 44.3 degrees, whereas the other three areas are relatively moderate with a maximum ground slope range of 18.5 degrees (Baltimore suburb). The point density stands for the number of lidar points per ten square meters which is calculated by the total number of lidar points divided by the entire area covered by the lidar data. As shown in Table 1, the point density varies from minimum 1.3 points (Baltimore downtown) to maximum 7.2 points (Toronto) per ten square meters in the four data sets. The number of ground points as the result of labeling operation is listed at the bottom of Table 1.

It should be noted that the ground spacing of lidar points is not even. As shown in Table 1, the ground spacing across track can be as twice smaller (Baltimore suburb) as the one in along-track. To illustrate and further examine this, Figure 2 presents and compares the distribution of samples points from suburban Baltimore and Osaka data sets. For the Baltimore data shown in Figure 2a, the ground spacing across track averaged about 2.3 meters, whereas the distance between two neighboring lidar profiles alternates with two different spacing intervals. The smaller along track spacing is at about 2.0 meters while the larger one is about 4.8 meters. Similarly, the Osaka data set shown in Figure 2b presents a similar pattern, though not as apparent as in the Baltimore dataset. This uneven spacing can be explained with the principles described by Wehr and Lohr (1999). The ground spacing across track is dependent on the laser pulse repetition frequency and the scan angle off the nadir. Therefore, the across track spacing can be treated as a constant in a small area as shown in Figure 2 and becomes larger at the swath boarder. Due to acceleration or slow-down of the scan mechanism, the points at the swath borders exhibit unwanted characteristics and are sometimes removed from the raw data set (Wehr and Lohr, 1999). As for the along-track ground spacing, it is determined by the airplane speed and the time period of one line scan. The bidirectional oscillating scanning causes a zigzag pattern with uneven distances along the flight direction. The ground spacing is smaller where the oscillating mirror finishes one scan line and changes its direction to start a new scan line, whereas it is larger between the start of one scan line and the end of the new scan line. This pattern repeats as shown in Figure 2. Because of this uneven distribution of lidar points in both along-track and across-track, we prefer using the term *point density* instead of *ground spacing* to describe the resolution of a lidar data set.

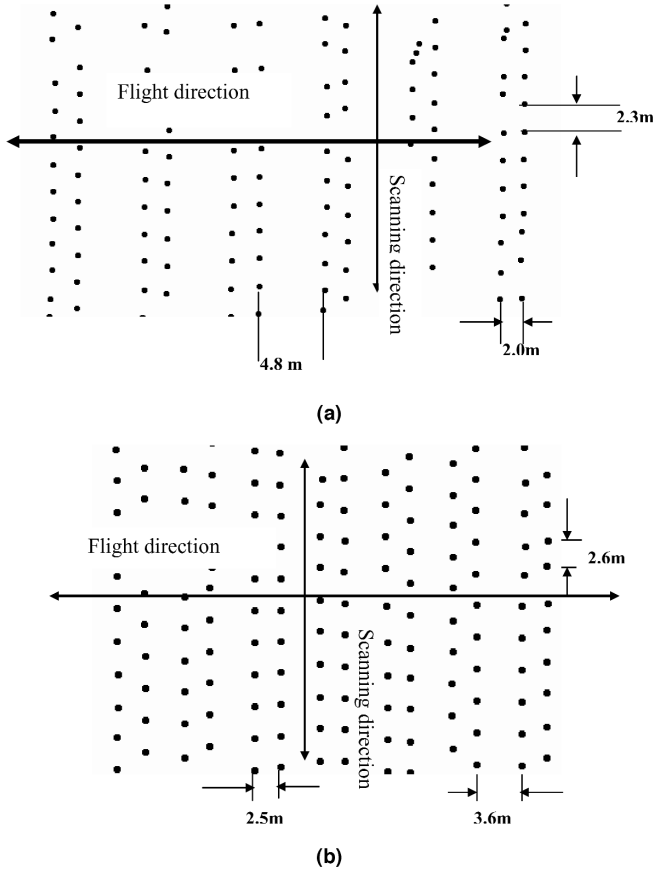

Figure 2. Point distribution and ground spacing: (a) Suburban Baltimore, and (b) Osaka.

One Dimensional, Bidirectional Labeling

In this section, we propose a filtering approach that has two sequential steps along the 1D lidar profile: labeling and adjustment. The labeling approach is based on both slope and elevation evaluation and implemented along the lidar profile in two opposite directions. A local linear regression along the lidar profile is then followed to further remove the possible non-ground points remaining from the previous step. This filtering process can be run multiple times if needed.

In order to eliminate non-ground points, the ground needs to be mathematically defined. Our definition is based on the slope between two consecutive points in a lidar profile as well as the elevation difference of a lidar point relative to its neighborhood in the profile. First, slopes at the border between non-ground (such as buildings) and ground are usually significantly larger than the ground slope at common lidar point density and continuous ground. Second, ground points have lower elevations than non-ground in the neighborhood. These two criteria are used to determine whether a lidar point is a ground point or a non-ground point. The slope criterion detects the edge points of buildings or other non-ground objects, such as bridges, vehicles, and trees. The elevation criterion considers the situation where the building roofs are not flat. When the building roof is complex and has many local changes in slope, using only the slope criterion may lead to erroneous results. The elevation criterion uses the fact that the elevation of a roof point is significantly higher than the ground elevation in its vicinity. Mathematically, we can express this observation as:

$$\forall P_i : \begin{cases} \text{if } (S_v > S_T \text{ and } Z_i > Z_T) \text{ non-ground point} \\ \text{otherwise ground point} \end{cases}. \quad (1)$$

This definition can be verbally described: for any lidar point P_i, if the slope S_v at its vicinity is greater than a given threshold S_T and its elevation Z_i is greater than a given threshold Z_T, then the point P_i is labeled as non-ground point; otherwise it will be labeled as ground point. Two criteria are considered in this formulation: slope and elevation. The check on the vicinity slope S_v essentially detects the presence of non-ground objects while the elevation condition determines if the lidar point belongs to the object or ground.

The implementation of the above criteria will affect the efficiency and performance of the DEM generation process. We propose a 1D, bidirectional labeling approach to separate ground from non-ground points based on the above criteria. First, the

slope S_i for lidar point P_i is calculated with two consecutive points along the lidar profile using the following equation

$$S_i = \arctan\left(\frac{Z_i - Z_{i-1}}{\sqrt{(X_i - X_{i-1})^2 + (Y_i - Y_{i-1})^2}}\right) \quad S_i \in \left[-\frac{\pi}{2}, \frac{\pi}{2}\right], \tag{2}$$

where $(X_{i-1}, Y_{i-1}, Z_{i-1})$ and (X_i, Y_i, Z_i) are the coordinates of two consecutive points in a lidar profile with Z coordinate pointing to the elevation direction and X, Y coordinates lying in the horizontal plane. Note the slope in Equation 2 can take both positive and negative signs. Point sequence entering a building from ground will get a positive (ascending) slope at the ground-building border while point sequence leaving a building will get a negative (descending) slope at the building-ground border. In our filtering approach, initially we assume the point sequence entering building from ground. Therefore, once a lidar point gets a slope greater than the given slope threshold S_T, it means the lidar profile reaches a building edge at this point. It will then be labeled as a non-ground point. The elevation and slope of the nearest detected ground point in the profile will be noted for prediction use. The algorithm continues labeling the subsequent points as building points until a negative slope is encountered. This negative slope (descending) point may possibly be a ground point and needs to be examined. We compare its elevation with the elevation of the nearest labeled ground point where the lidar profile reached the building. If the two elevations are close within an established tolerance, the algorithm labels the descending point as ground which means the lidar profile leaves the building and returns to ground at this point. This method works well when the topography is relatively flat. For hilly regions, prediction is needed. We use the slope of the nearest ground point to predict the elevation of the descending point. If the elevation of the descending point is higher than the predicted one, it will still be labeled as building, otherwise the lidar profile leaves the building and returns to ground. This labeling process continues until the last lidar point in the file. This is regarded as the *forward labeling* process. To consider the situation when the first lidar point in the file is a non-ground point, we repeat the above process in the reverse direction by starting the labeling process from the last point in the data set, namely the backward labeling process. The resultant non-ground points are then the union of the two labeling processing results, whereas the resultant ground points are equivalently the intersection of the two labeling process results.

After the forward and backward labeling, a 1D linear regression is carried out to further remove possible remaining non-ground points in the labeled ground points. This assumes that the local topography of a certain neighborhood in the lidar profile can be expressed as an equal slope Z-profile, namely

$$Z = a_0 + a_1 D \qquad D < D_T, \tag{3}$$

where a_0, a_1 are the coefficients of the local Z-profile, D is the distance between lidar points within the neighborhood which is defined by a given distance threshold D_T. Points within the window will be used to determine the local Z-profile based on the least squares regression. Points that have more than three times of the standard deviation of the regression will be removed as non-ground points.

The entire labeling process is illustrated step-by-step in Figure 3 by a lidar profile of approximately 250 meters long in suburban Baltimore. Figure 3a plots the original lidar points. Figure 3b and 3c are respectively the ground points obtained from the forward (from right to left) and backward (from left to right) labeling processes. The combination (intersection) of these two is shown in Figure 3d, which is further filtered by the 1D linear regression. The final result is shown in Figure 3e. As shown in Figure 3b and 3c, either forward or backward processing can correctly label almost all ground points and most building points. However, each step mistakenly labels several building points as ground points. It is noticed that these two wrongly labeled point sets have almost no common points (Figure 3b and 3c). Therefore, keeping the points that are both labeled as ground points in the forward and backward processes will correct the falsely identified ground points. The combined result is shown as in Figure 3d. The final 1D regression further filters possible building points and keeps all ground points as shown in Figure 3e. Figure 4 illustrates the same process, however, in a 3D perspective view, where lidar points are overlaid atop the lidar surface model. As shown in Figure 4, the labeling process in one direction, either forward or backward, may detect more building points than the other. In this example, the backward labeling identifies most building points. The combination of the forward and backward labeling detects almost all building points, except some points on one long building at the upper left portion of the 3D view in Figure 4. Satisfactory results are obtained after applying the 1D linear regression. No obvious building points are left in the resultant ground model. A visual check in Figure 4e also reveals that building edges are well identified and no apparent ground points are labeled as building points.

The proposed approach has a few distinctions. First, it is computationally efficient as the calculation is performed within the 1D lidar profile. For the slope calculation in Equation 2, only two consecutive points are needed. The local elevation and slope are updated every time a building is encountered along the profile and adapts itself in accordance to the topography of the area. Moreover, for the final 1D linear regression, a window of lidar profile is needed. Because the raw lidar data is at irregular interval and stored as a sequence of sample points, the only explicit topologic relationship is the neighborhood of two consecutive points along a profile. By taking advantage of this, the proposed algorithm does not require any preprocessing to form a special data structure, such as TIN or a grid, to facilitate the filtering process. It needs no searching or calculation outside a lidar profile. In this way, the required computations are reduced to minimum, which will substantially increase the efficiency in handling large volume lidar data for practical applications.

Second, the use of the raw lidar data instead of its interpolated values, e.g., a regular grid, assures the calculated slopes rigorously reflect the local elevation change. This is because the calculation is undertaken for all consecutive sample points along the profile in the raw data, and no smoothing or interpolation operation is involved. Therefore, no artificial points are introduced in the calculation as it would if interpolation were used. In this way, using raw lidar data avoids a potential meaningless operation of judging whether a non-existent point generated during the interpolation process is a ground or non-ground point.

Third, the combination of slope and elevation criteria can consider the complexity of building architecture. As addressed earlier, the slope criterion essentially detects the ground-building edge while the elevation criterion identifies the roof points within a building region. The selection of the local ground elevation threshold is adaptive. Each time a building is encountered, the elevation of the nearest ground point is then chosen as the elevation threshold. When the terrain has extreme relief, the nearest ground slope is used to predict the ground elevation on the other side of the building. In this way, the approach is adaptive to terrain type and building complexity, and we avoid the difficulty to handle the fact that anything can occur at any elevation.

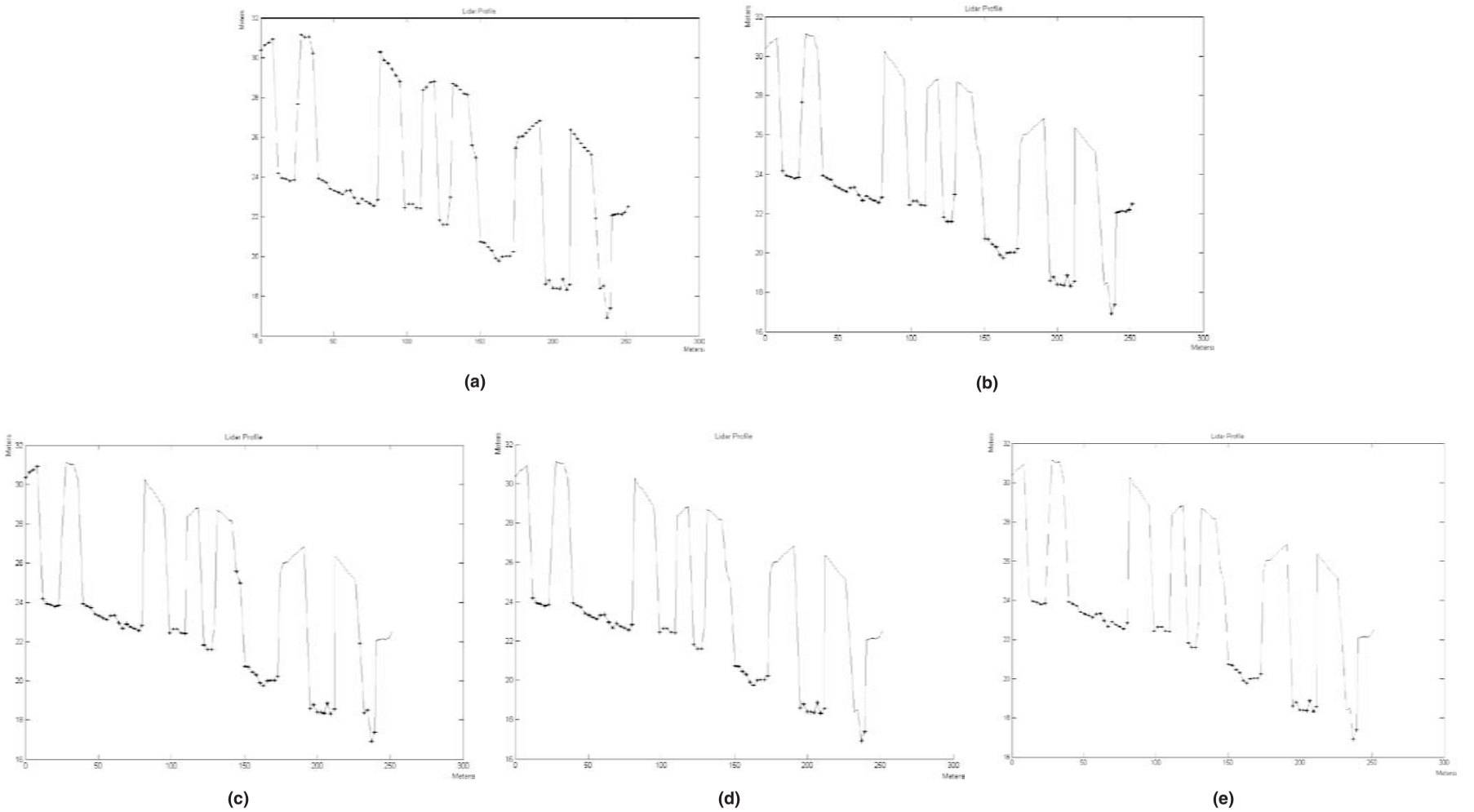

Figure 3. Stepwise profile illustration of the labeling approach (Suburban Baltimore): (a) Original lidar points, (b) Ground points from forward (from right to left) labeling, (c) Ground points from backward (from left to right) labeling, (d) Combination of forward and backward labeling, and (e) Final ground points after regression.

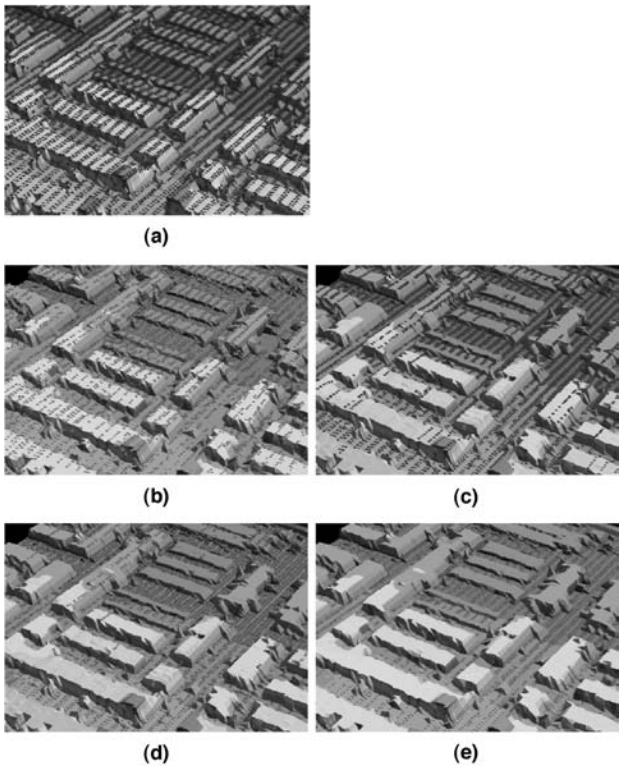

Figure 4. Stepwise 3D illustration of the labeling process (Suburban Baltimore): (a) Raw data. (b) Ground points from forward labeling, (c) Ground points from backward labeling, (d) Ground points after forward, and backward labeling, and (e) Final ground points after regression.

Finally, the bidirectional labeling process avoids the potential vulnerability of the filtering operation. If a labeling process starts with lidar points on relatively flat roofs, the building may not be correctly detected. All the roofs points in that building would be mistakenly labeled as ground points (see Figure 3b). However, the labeling process in the reverse direction will enable the labeling sequence enter the building from ground which means the ground-building edge will be correctly determined. Therefore, the missed buildings in the first labeling step will be identified in the second labeling step from the opposite direction (see Figure 3c). Through this bidirectional labeling process, the reliability of the filtering operation is assured.

Results and Assessment

The proposed filtering approach is implemented to four urban data sets. The test areas are mixed with buildings and other urban objects. A 30 degree slope threshold is chosen for all data sets except Toronto. The Toronto data have higher point density and complex topography, such as, cliffs or large ramps towards the northern edge of the area. The labeling process repeats twice in this case. A relative large slope threshold of 70 degrees is given to remove buildings and sparse tree canopy in the first filtering. In the second filtering, a relative smaller slope threshold of 40 degrees is chosen mainly to remove the vehicles on the streets.

To quantitatively assess the labeling results, a number of homogenous ground and building regions defined by polygons are selected as ground truth in each data set. The polygons are manually delineated over the lidar data coded by elevation and evenly distributed in the study area as shown in Figure 1, where building and ground polygons are shown in black and white, respectively. The number of delineated building and ground polygons is listed in Table 2.

Labeling results are compared with the selected ground truth to conduct the assessment. The ground truth is obtained by counting the number of raw lidar points inside the selected building and ground polygons, respectively. The counting results are shown under the "Ground truth" columns in Table 2. For the labeling results, however, the building points may be wrongly labeled as ground points while the ground points may be wrongly labeled as building points. Therefore, both building points and ground points in the labeling results need to be counted against the ground truth polygons. The counting results are listed under "Labeling results" columns in Table 2. Rows in Table 2 under "Labeling results" contain the number of points and their percentage (within parentheses) that are either correctly or wrongly labeled for each study area. As a general assessment, the overall labeling results for all the four study areas are listed at the bottom of the table which essentially is an average performance measure.

Table 2 is used to evaluate the performance of the proposed labeling approach. A comparison on the number of points counted from labeling results and the ground truth will serve this purpose. As is shown in Table 2, for the ground regions, an average 97.3 percent of the total points are correctly labeled. Accordingly, the mislabeling rate for ground points (false negative rate, wrongly labeled as building) is about 2.7 percent in average. For building regions, the average correct labeling rate

TABLE 2. QUALITY OF THE LABELING ALGORITHM

	Ground Truth			Labeling Results	
Site Name	Point Type	# of Regions	# of Points	Ground (# and %)	Building (# and %)
Baltimore Suburb	Ground	18	1692	1645 (97.2)	47 (2.8)
	Building	22	4012	21 (0.5)	3991 (99.5)
Baltimore Downtown	Ground	19	1784	1747 (97.9)	37 (2.1)
	Building	24	8081	122 (1.5)	7959 (98.5)
Osaka	Ground	15	3069	3036 (98.9)	33 (1.1)
	Building	14	4668	72 (1.5)	4596 (98.5)
Toronto	Ground	14	3387	3234 (95.5)	153 (4.5)
	Building	15	9282	455 (4.9)	8827 (95.1)
Overall (Average)	Ground	66	9932	9662 (97.3)	270 (2.7)
	Building	75	26043	670 (2.6)	25373 (97.4)

is 97.4 percent, with an average false positive (wrongly labeled as ground) rate 2.6 percent. These quantities can be understood as the overall performance of the proposed approach. The similar error rates (2.6 percent versus 2.7 percent) of the two possible mistakes suggest a good balance is achieved in the algorithm's performance. Table 2 also suggests that the performance of the labeling approach varies with the topographic complexity. The study areas of Baltimore suburb and downtown, and Osaka are relatively flat as listed in Table 1. Their labeling error rate ranges from 0.5 percent (Baltimore suburb, false positive) to 2.1 percent (Baltimore urban, false negative). For the Toronto area, cliffs or large ramps exist as shown in Figure 8 and Figure 10d. Their labeling error rates may increase to 4.9 percent (false positive) and 4.5 percent (false negative), respectively.

Figure 5 and 6 respectively present selected 2D and 3D views of the labeling results for the four study areas. In the 2D views available orthoimages produced from digital images collected during the lidar flight are also shown for the two Baltimore data sets. Both figures show ground points in black and non-ground points in white. All results in Figure 5 and 6 exhibit that all buildings, including the complex roofs and side architectures, can be correctly identified. A closer examination of the results in Baltimore suburban and Osaka (Figure 5a, 5c) suggests the approach can also successfully label individual trees and vehicles in relatively open areas. Figure 5b and 5d show less successful, yet still quite satisfactory, labeling results in highly urban areas. Almost all vehicles in the surface parking area in the middle of in Figure 5b are correctly labeled. However, some ground points on the horizontal street at the bottom of Figure 5b are mistakenly labeled as

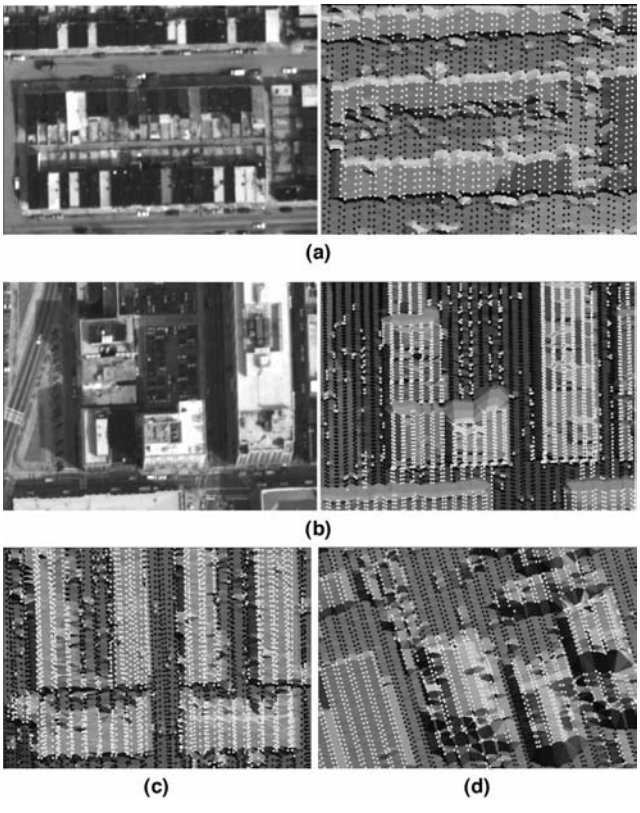

Figure 5. Labeling results (ground: black; non-ground: light): (a) Ortho image (left) and labeling results (right) in Suburban Baltimore, (b) Ortho image (left) and labeling results (right) in Downtown Baltimore, (c) Osaka, and (d) Toronto.

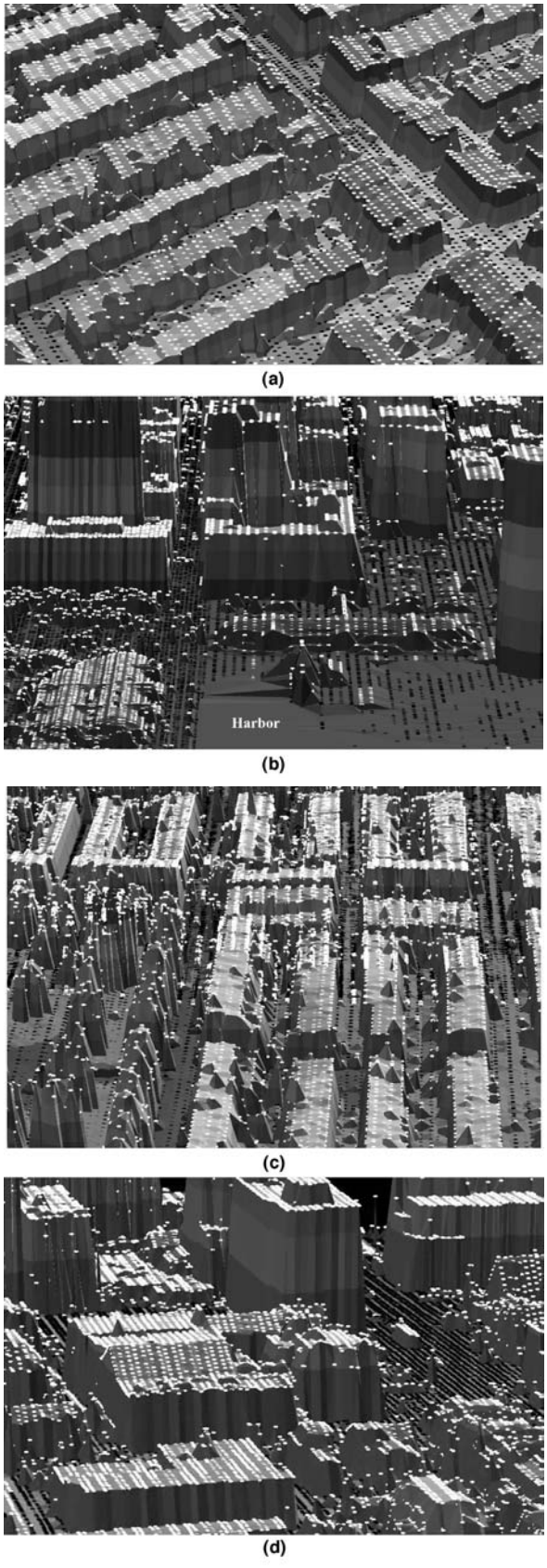

Figure 6. 3D view of labeling results (ground: black; non-ground: white): (a) Suburban Baltimore, (b) Downtown Baltimore, (c) Osaka, and (d) Toronto.

non-ground, as a trade-off that many vehicles on that street are identified correctly. The 3D views in Figure 6 provide a clear perception that complex buildings, trees and vehicles, which appear to be bumps in the 3D view, are correctly labeled.

Figure 7 is several selected closer examinations for handling typical urban man-made features. Shown in this figure are complex buildings, bridges, trees, and water body (harbor) along with their orthophoto images from the Baltimore downtown data. Notice that the two small concave parts in the middle left and right of Figure 7a are not identical in height. The left is ground, while the right is part of the building. The algorithm successfully detects this, which is then verified by manually measuring their elevation and comparing it with the vicinity ground. Figure 7b shows the labeling of a likely ring-shape building. The labeling process identifies the inner part as building other than ground which is further verified by manual check. Notice the black object on the roof does not produce any return; the lidar data are void in this part. However, this does not cause problem in the labeling algorithm, Figure 7c attempts to demonstrate the capability of labeling bridges as non-ground. As is shown, all three bridges are correctly labeled. The labeling of the water body is shown in Figure 7d. The returns from water surface or its objects are very sparse. Because of its flat surface, water and the deck are labeled as ground. To ultimately determine the thematic nature of those labels, only using spatial information in the lidar data may not be sufficient. Spectral information from images can be of great help to intercept these features.

Figure 8 and 9 examine the labeling performance for discontinuity areas of ground elevation in the Toronto data set. Presented in Figure 8 is a ramp or cliff of sudden and large elevation change. As is shown in Figure 8, the ramp is likely covered by trees or bushes. Points with high slopes in the ramp are labeled as non-ground while others are labeled as ground. Due to the dense canopy coverage, many points in the ramp are filtered out as no-ground points. As a result of this, the final DEM for the ramp is greatly smoothed as shown in Figure 10d. It is also shown that all complex buildings are correctly labeled; so are the most vehicles on the streets.

A singular situation (outlier) occurs when the ground has a *sink*. As shown in Figure 9, for unknown reasons the ground shows single-point sinks. The individual sinks are correctly labeled as ground, however, the vicinity ground may possibly wrongly labeled as non-ground. To avoid this over-filtering (ground wrongly labeled as a building), we restrict the number of labeled consecutive non-ground points to a limit. This limit corresponds to the possible maximum length of a building, which is chosen as 200 meters in this study. In this way, the mislabeling, if it occurs, will be limited to a certain extent other than deteriorate the entire results. Areas with such *sinks* may need special treatment as discussed in (Masaharu and Ohtsubo, 2002).

As the final outcome, Figure 10 presents 3D shaded relief of the DEM generated using the labeled ground points. The number of ground points used is listed in Table 1. The DEM grids are generated using natural-neighbor (Watson and Phillip, 1987) interpolation method at a cell size of one meter, and the elevation exaggeration factor is 2.5. Since the DEM is shaded according to the slope, terrain relief change is magnified. Comparing to 3D perspective views, the shaded relief provides a better and exaggerated way to visually examine the quality of filtering operation. As is shown in Figure 10, the generated DEM reflect the natural relief of the areas. No large man-made objects are visible. However, speckle-type artifacts exit in the final DEM. They are typically caused by individual points returned from trees and vehicles remaining from the labeling process. It should be noted that the speckle offsets are very

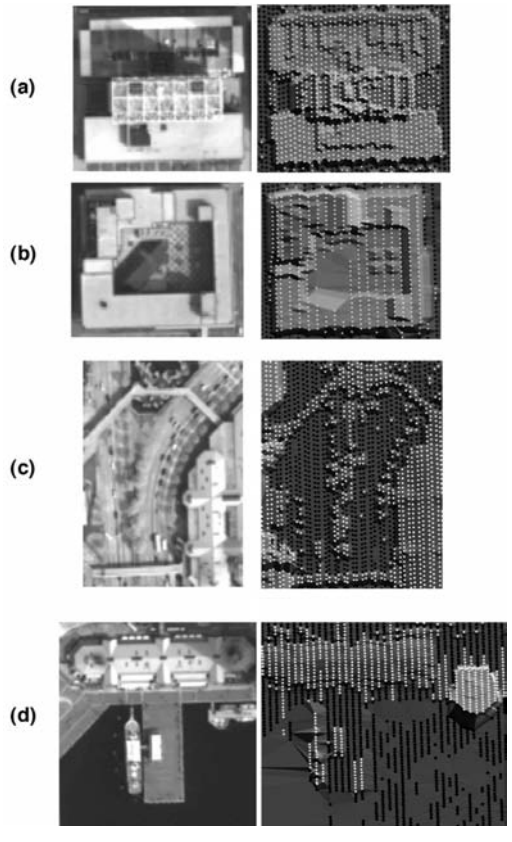

Figure 7. Orthophoto image (left) and labeling results (right) in Baltimore: (a) Building 1, (b) Building 2, (c) Bridges and trees, and (d) Water.

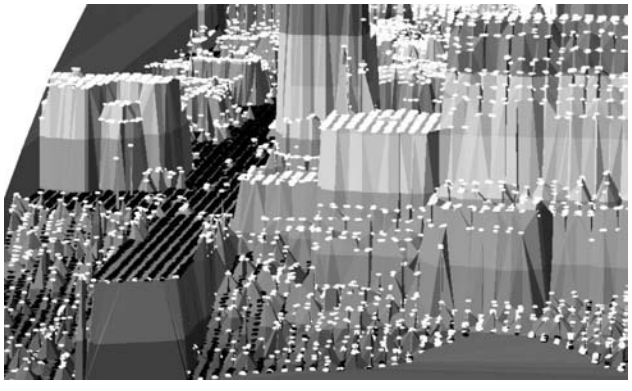

Figure 8. Steep terrain with trees (Toronto).

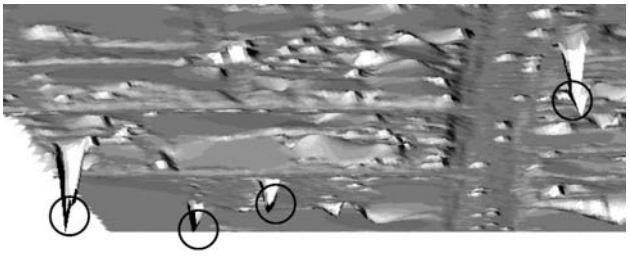

Figure 9. Ground sinks (Looking from underground, Toronto).

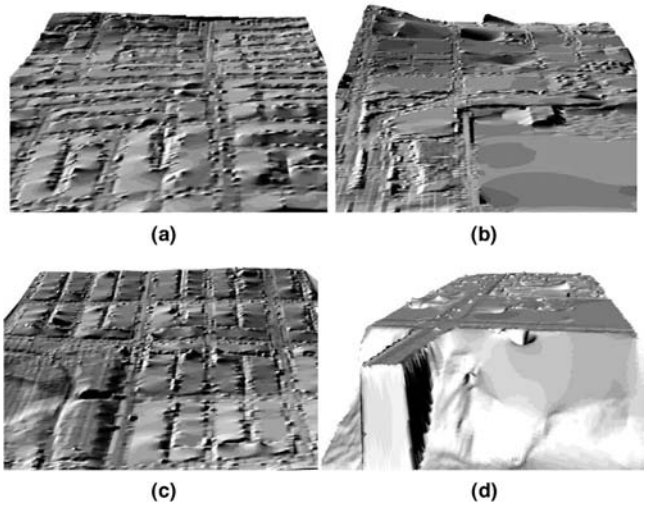

Figure 10. Shaded ground relief (elevation exaggeration factor of 2.5) for: (a) Suburban Baltimore, (b) Urban Baltimore, (c) Osaka, and (d) Toronto.

small. Almost all of them are within one meter above the ground. As estimated above, such error rate is maximum 4.9 percent (Toronto) as a trade-off of balancing the two types of labeling mistakes.

Conclusions

Generating the bald ground DEM from raw lidar data requires a mathematic formulation, which should consider both slope and elevation criteria. The slope criterion detects the presence of non-ground objects, while the elevation criterion determines if the lidar points belong to an object or ground. The proposed labeling approach is computationally efficient and reliable because of its 1D bidirectional implementation. The adaptive thresholding technique based on local topography makes this approach applicable to a variety of urban areas with different building complexity and terrain relief.

The proposed approach can provide satisfactory DEM in complex urban environments. Most urban features, such as complex buildings, bridges, vehicles, and trees can be correctly separated from ground. Difficulty may occur at places being full of vehicles or trees, and vehicle-present streets and objects (such as a bridge) that have a small slope change along the lidar scan line. The complete separation of water from ground may need spectral information. Quality assessment based on ground truth suggests that an optimal filtering approach essentially needs to achieve the best balance of the false positive and false negative errors. The proposed labeling approach exhibits an average 2.6 percent false positive and 2.7 percent false negative mislabeling rates over the four study areas. These error rates increase when the topography has larger range of ground slopes. Further effort will be made to detect and remove very small artifacts remaining from the labeling process and to use imagery along with lidar data for a complete separation of ground features.

Acknowledgments

The Baltimore data were provided by EarthData Technologies, Maryland. The Osaka and Toronto data were provided by Optech, Inc., Toronto, Canada.

References

Ackermann, F., 1999. Airborne Laser Scanning—Present Status and Future Expectations, *ISPRS Journal of Photogrammetry and Remote Sensing*, Vol. 54, Issues 2–3, July, pp. 64–67.

Axelsson, P., 1999. Processing of laser scanner data—algorithms and applications, *ISPRS Journal of Photogrammetry and Remote Sensing*, Vol. 54, Issues 2–3, July, pp. 138–147.

Axelsson, P., 2000. DEM Generation from Laser Scanner Data Using Adaptive TIN Models, *International Archive of Photogrammetry and Remote Sensing*, Vol. XXXIII, Part B4, pp. 110–117.

Baltsavias, E., 1999. A Comparison Between Photogrammetry and Laser Scanning, *ISPRS Journal of Photogrammetry and Remote Sensing*, Vol. 54, Issues 2–3, July, pp. 83–94.

Crombaghs, M., S.O. Elberink, R. Brügelmann, and E. de Min, 2002. Assessing Height Precision of Laser Altimetry DEMs, *International Archives of the Photogrammetry, Remote Sensing and Spatial Information Sciences*, Vol. XXXIV Part 3A, Commission III, September 9–13, Graz, Austria, pp. 85–90.

Elmqvist, M., 2002. Ground Surface Estimation from Airborne Laser Scanner Data Using Active Shape Models, *International Archives of the Photogrammetry, Remote Sensing and Spatial Information Sciences*, Vol. XXXIV Part 3A, Commission III, 09–13, September, Graz, Austria, pp. 115–118.

Fowler, R., 2001. *Topographic Lidar, in Digital Elevation Model Technologies and Applications: The DEM Users Manual*, David F. Maune, Editor, The American Society for Photogrammetry and Remote Sensing, Bethesda, Maryland, USA, 539 pages.

Haugerud, R.A., and D.J. Harding, 2001. Some Algorithms for Virtual Deforestation (VDF) of Lidar Topographic Survey Data, *Proceedings of the ISPRS workshop on Land Surface Mapping and Characterization Using Laser Altimetry, Annapolis, Maryland,* The International Archives of the Photogrammetry, Remote Sensing and Spatial Information Sciences, Vol. XXXIV Part 3/W4 Commission III, pp. 203–209.

Huising, E.J., and L.M. Gomes Pereira, 1998. Errors and accuracy estimates of laser data acquired by various laser scanning systems for topographic applications, *ISPRS Journal of Photogrammetry and Remote Sensing*, Vol. 53, Issue 5, October, pp. 245–261.

Kilian, J., N. Haala, and M. English, 1996. Capture and Evaluation of Airborne Laser Scanner Data, *International Archives of Photogrammetry and Remote Sensing*, Vol. XXXI, Part B3, Vienna, pp. 383–388.

Knabenschuh, M., and B. Petzold, 1999. Data Post-processing of Laser Scan Data for Countrywide DEM Production, *Proceedings of the Photogrammetry Week*, D. Fritsch and R. Spiller, Editors, pp. 233–240.

Kraus, K., and N. Pfeifer, 1998. Determination of Terrain Models in Wooded Areas with Airborne Laser Scanner Data, *ISPRS Journal of Photogrammetry and Remote Sensing*, Vol. 53, Issue 4, August, pp. 193–203.

Kraus, K., and N. Pefifer, 2001. Advanced DEM Generation from Lidar Data, *Proceedings of the ISPRS workshop on Land Surface Mapping and Characterization Using Laser Altimetry* (Hofton, M., editor), Annapolis, Maryland, The International Archives of the Photogrammetry, Remote Sensing and Spatial Information Sciences, Vol. XXXIV, Part 3/W4 Commission III.

Lindenberger, J., 1993. Laser-Profilmessungen zur topographischen Gelaedeaufnahme, *Deutsche Geodaetische Kommission*, Series C, No. 400, Munich. (In German)

Masaharu, H., and K. Ohtsubo, 2002. A Filtering Method of Airborne Laser Scanner Data for Complex Terrain, *International Archives of the Photogrammetry, Remote Sensing and Spatial Information Sciences*, Vol. XXXIV Part 3B, Commission III, 09–13, September, Graz, Austria, pp. 165–169.

Petzold, B., P. Reiss, and W. Stoessel, 1999. Laser Scanning—Surveying and Mapping Agencies are Using a New Technique for the Derivation of Digital Terrain Models, *ISPRS Journal of Photogrammetry and Remote Sensing*, Vol. 54, Issues 2–3, July, pp. 95–104.

Raber, G.T., J.R. Jensen, S.R. Schill, and K. Schuckman, 2002. Creation of Digital Terrain Models Using an Adaptive Lidar Vegetation Point Removal Process, *Photogrammetric Engineering & Remote Sensing*, Vol. 68, No. 12, pp. 1307–1316.

Schickler, W., and A. Thorpe, 2001. Surface estimation based on Lidar, *Proceedings of the ASPRS Annual Conference*, 23–27, April, St. Louis, Missouri, unpaginated CD-ROM.

Sithole, G., 2001. Filtering of Laser Altimetry Data Using a Slope Adaptive Filter, *Proceedings of the ISPRS workshop on Land Surface Mapping and Characterization Using Laser Altimetry* (Hofton, M., editor), Annapolis, Maryland, The International Archives of the Photogrammetry, Remote Sensing and Spatial Information Sciences, Vol. XXXIV Part 3/W4 Commission III, pp. 203–210.

Sithole, G., 2002. Filtering Strategy: Working Towards Reliability, *International Archives of the Photogrammetry, Remote Sensing and Spatial Information Sciences*, Vol. XXXIV Part A3, Commission III, 09–13, September, Graz, Austria, pp. 330–335.

Vosselman, G., 2000. Slope Based Filtering of Laser Altimetry Data, *International Archives of Photogrammetry and Remote Sensing*, Vol. XXXIII, Part B3, Amsterdam 2000, pp. 935–942.

Vosselman, G., and H. Mass, 2001. Adjustment and Filtering of Raw Laser Altimetry Data, *Proceedings OEEPE Workshop on Airborne Laserscanning and Interferometric SAR for Detailed Digital Elevation Models*, March 1–3, Stockholm.

Wang, Y., B. Mercer, C., Tao, J. Sharma, and S. Crawford, 2001. Automatic Generation of Bald Earth Digital Elevation Models from Digital Surface Models Created Using Airborne IFSAR, *Proceedings of the ASPRS Annual Conference*, April 23–27, St. Louis, Missouri, unpaginated CD-ROM.

Wack, R., and A. Wimmer, Digital Terrain Models from Airborne Laserscanner Data—a Grid Based Approach, *International Archives of the Photogrammetry, Remote Sensing and Spatial Information Sciences*, Vol. XXXIV Part 3B, Commission III, 09–13, September, Graz, Austria, pp. 293–296.

Watson, D.F., and G.M. Phillip, 1987. Neighbor Based Interpolation, *Geobyte*, Vol. 2, No. 2, pp. 12–16.

Wehr, A., and U. Lohr, 1999. Airborne Laser Scanning—an Introduction and Overview, *ISPRS Journal of Photogrammetry and Remote Sensing*, Vol. 54, Issues 2–3, July, pp. 68–82.

Yoon, J.S., and J. Shan, 2002. Urban DEM Generation from Raw Airborne Lidar Data, *Proceedings of the Annual ASPRS Conference*, Washington, D.C., April 22–26, unpaginated CD-ROM.

Zinger, S., M. Nikolova, M. Roux, and H. Maître, 2002. 3D Resampling for Airborne Laser Data of Urban Areas, *International Archives of the Photogrammetry, Remote Sensing and Spatial Information Sciences*, Vol. XXXIV Part A3, Commission III, September 9–13, Graz, Austria, pp. 418–423.

(Received 08 July 2003; accepted 25 September 2003; revised 08 October 2003)